

# DESIGN OF NOVEL PERMANENT MAGNET BIASED LINEAR MAGNETIC BEARING AND ITS APPLICATION TO HIGH-PRECISION LINEAR MOTION STAGE

**Sang-Ho Lee**

School of Mechanical and Aerospace Eng., Seoul National Univ., Seoul, 151-742, Korea  
sang.ho.lee@samsung.com

**Jeeuk Chang**

School of Mechanical and Aerospace Eng., Seoul National Univ., Seoul, 151-742 Korea  
garnet@amed.snu.ac.kr

**Sang-Wook Lee**

Dept. of Mechanical & Industrial Eng., Univ. of Illinois at Urbana-Champaign,  
Champaign, IL 61801, USA  
slee@uiuc.edu

**Oui-Serg Kim**

School of Mechanical and Aerospace Eng., Seoul National Univ., Seoul, 151-742 Korea  
oskim@amed.snu.ac.kr

**In-Bae Chang**

Kangwon National Univ., Chun-chon, 200-701 Korea  
inbae@kangwon.ac.kr

**Dong-Chul Han**

School of Mechanical and Aerospace Eng., Seoul National Univ., Seoul, Pref., 151-742 Korea  
dchan@amed.snu.ac.kr

## ABSTRACT

This paper provides a development of a new permanent magnet biased linear magnetic bearing (PMMB) and its application to the magnetically levitated (maglev) high-precision linear motion stage. The basic concept and theoretical equations of the novel permanent magnet biased linear magnetic bearing are presented, and its characteristics are verified by various experiments using a 1-DOF test rig. The high-precision maglev motion stage supported by four bearing modules is built and operated with 50nm precision of the positioning errors.

## NOMENCLAUTURE

$N$  : coil turns  
 $I$  : current  
 $B_r$  : remnant magnetic flux density of PM  
 $\mu_m$  : relative permeability of PM  
 $\mu_0$  : permeability of air  
 $l_m$  : thickness of PM  
 $g_0$  : nominal gap size between core and guide  
 $x$  : displacement of magnetic bearing  
 $\phi_1, \phi_2$  : magnetic flux  
 $A_g$  : area of pole  
 $A_m$  : area of permanent magnet  
 $B_1, B_2$  : magnetic flux density in upper and lower gap  
 $F$  : force of magnetic bearing  
 $K_x$  : displacement stiffness

$K_I$  : current stiffness

$m$  : magnetic bearing unit mass

$\Delta m$  : additional mass to magnetic bearing unit

$B_{nom}$  : nominal magnetic flux density in  $x=0, I=0$

## INTRODUCTION

Various researches on the high-precision maglev motion stage supported by the active magnetic bearing (AMB) have been performed with its advantages such as: non-contact motion, the possibility of operation in vacuum and active compensation of the traveling errors which caused by the geometric errors and misalignment of the support guides. However, aside from the static current to support the stage's own weight, a large amount of bias current is required to increase the dynamic stiffness of the stage and to linearize the current-magnetic force relationship. The usage of a large amount of bias current will decrease the whole system's efficiency and cause the excessive heat generation problem that degrades the repeatability of the system and makes the size of each magnetic bearing and whole maglev stage bulky. The thermal deformation analysis and compensation techniques are required to build a high-precision system using electromagnetic bearings. Moreover some advanced control techniques, such as a nonlinear control and compensation are required because nonlinear displacement-current relationship of the electromagnets

cannot be removed even if we use the bias linearization method. The linearity in wide operating range is one of the important requirements of the actuators for the high-precision stages, which can adjust the large traveling errors induced while the stage travels along the support guides. Thus in this paper a new AMB which use permanent magnet instead of bias current is designed and tested in 1-Dof test rig and 6-Dof stage.

## PERMANENT MAGNET BIASED LINEAR MAGNETIC BEARING

### Idea of PMMB

The structure of PMMB is shown in Figure 1. There are three I-shaped cores between two fixed guides and the permanent magnet (PM) is positioned with same magnet pole faced. Coil is wound on the I shaped core of center. Assembled body of three I-shaped cores, two PMs and coil is levitated.

Magnetic field of PM is formed symmetrically along black arrows in Figure 1. But Magnetic field of electromagnet (EM) has the same direction as that of PM in upper part and opposite direction in lower part. The difference between the two magnetic field density makes a levitation force. So we can get a magnetic force equation of PMMB.

$$B_u = B_{u,pm} + B_{em} \quad (1)$$

$$B_l = B_{l,pm} - B_{em}$$

$$F = \frac{1}{2\mu_0} (B_u^2 - B_l^2) (4A_g) \quad (2)$$

Superposed flux lines are shown in Figure 2. Left one is flux lines of PM only, center one is that of only EM and right one is the sum of both flux. Since the thickness of PM is wider than the total gap in path of EM flux, flux of EM does not penetrate PM. Thus the performance degradation resulted from demagnetization can be ignored.

### Magnetic Circuit

Since PMMB is symmetric, we use half magnetic circuit model in Figure 3 for analysis. Because permeability of core is larger than that of the gap, we ignore magnetic resistances of cores and ignore nonlinear characteristics and the leakage. Maxwell equation of magnetic circuit in Figure 3 makes,

$$\begin{bmatrix} \mu_0 NI + \frac{B_r \cdot l_m}{\mu_m} \\ \mu_0 NI - \frac{B_r \cdot l_m}{\mu_m} \end{bmatrix} = \begin{bmatrix} 2 \frac{g_0 - x}{A_g} + \frac{l_m}{\mu_m A_m} & -\frac{l_m}{\mu_m A_m} \\ -\frac{l_m}{\mu_m A_m} & 2 \frac{g_0 + x}{A_g} + \frac{l_m}{\mu_m A_m} \end{bmatrix} \begin{bmatrix} \phi_1 \\ \phi_2 \end{bmatrix} \quad (3)$$

$$= \begin{bmatrix} 2(g_0 - x) + \frac{l_m}{\mu_m} \cdot \frac{A_g}{A_m} & -\frac{l_m}{\mu_m} \cdot \frac{A_g}{A_m} \\ -\frac{l_m}{\mu_m} \cdot \frac{A_g}{A_m} & 2(g_0 + x) + \frac{l_m}{\mu_m} \cdot \frac{A_g}{A_m} \end{bmatrix} \begin{bmatrix} B_1 \\ B_2 \end{bmatrix}$$

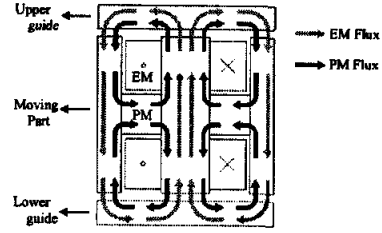


FIGURE 1: Permanent magnet biased linear magnetic bearing

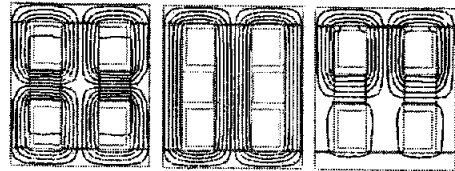


FIGURE 2: Flux lines of permanent magnet biased linear magnetic bearing

Left: PM, Middle: EM, Right: superposed

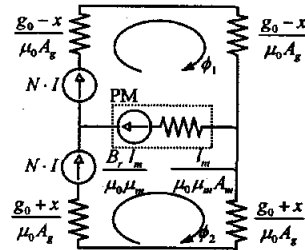


FIGURE 3: Equivalent magnetic circuit

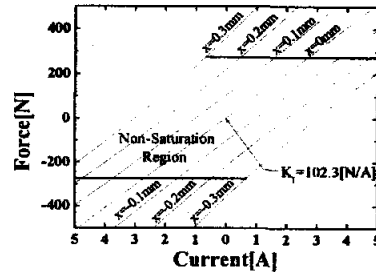


FIGURE 4: Calculated magnetic force vs. current

Magnetic field density  $B_1, B_2$  and magnetic force  $F$  of PMMB is obtained.

$$\begin{bmatrix} B_1 \\ B_2 \end{bmatrix} = \frac{1}{2 \left( g_0^2 - x^2 + \frac{l_m}{\mu_m} \cdot \frac{A_g}{A_m} g_0 \right)} \times \begin{bmatrix} \left( g_0 + x + \frac{l_m}{\mu_m} \cdot \frac{A_g}{A_m} \right) \mu_0 NI + (g_0 + x) \cdot \frac{B_r \cdot l_m}{\mu_m} \\ \left( g_0 - x + \frac{l_m}{\mu_m} \cdot \frac{A_g}{A_m} \right) \mu_0 NI - (g_0 - x) \cdot \frac{B_r \cdot l_m}{\mu_m} \end{bmatrix} \quad (4)$$

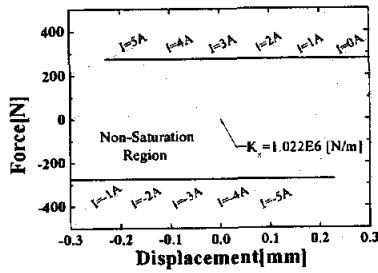


FIGURE 5: Calculated magnetic force vs. displacement

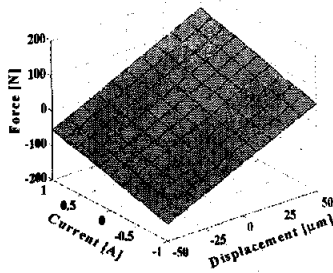


FIGURE 6: Calculated force by Finite Element Method

TABLE 1: Specification of the PMMB

Magnet dimension	NdFeB	
remnant flux density	20×10×10	(mm <sup>3</sup> )
	1.05	(T)
Core dimension	41×6×0.35	(mm <sup>3</sup> )
Total pole area	480	(mm <sup>2</sup> )
Coil turns	105×2	
Nominal gap	0.325	(mm)

$$F = \frac{1}{2\mu_0} (B_1^2 \cdot (4A_g) - B_2^2 \cdot (4A_g)) = \frac{2}{\mu_0} (B_1^2 - B_2^2) \cdot A_g$$

$$= \frac{2}{\mu_0} [B_1 \quad B_2] \cdot \begin{bmatrix} A_g & 0 \\ 0 & -A_g \end{bmatrix} \cdot \begin{bmatrix} B_1 \\ B_2 \end{bmatrix} \quad (5)$$

In Figure 4 and 5, the magnetic force has highly linear characteristics about coil current and displacement of levitated target. It has 1% or fewer non-linearity in operating range of  $\pm 2A$ ,  $\pm 100\mu m$ . Compared to the nonlinear characteristics of EM<sup>(5)</sup>, PMMB has wide operating range. So a new PMMB is easy to control and compensate positioning error.

In linearized equations, current stiffness and displacement stiffness is obtained by differentiating magnetic force  $F$  with respect to  $x$  and  $I$  respectively.

$$F = K_x \cdot x + K_I \cdot I$$

$$K_x = \frac{\partial F}{\partial x} \Big|_{x=0, I=0} = \frac{2A_g B_r^2}{\mu_0 g_0 \left( \mu_m \cdot \frac{g_0}{l_m} + \frac{A_g}{A_m} \right)^2} \quad (6)$$

$$K_I = \frac{\partial F}{\partial I} \Big|_{x=0, I=0} = \frac{2NA_g B_r}{g_0 \left( \mu_m \cdot \frac{g_0}{l_m} + \frac{A_g}{A_m} \right)}$$

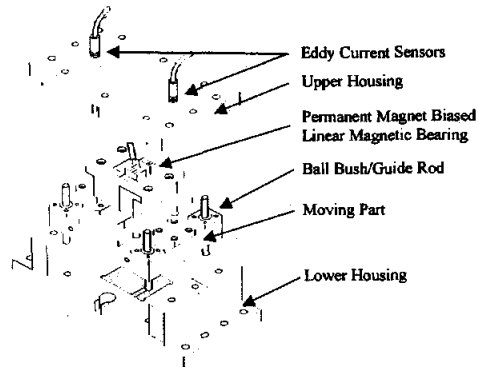


FIGURE 7: Schematics of the 1-Dof test rig

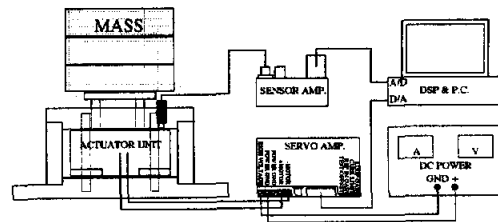


FIGURE 8: System configuration of the 1-Dof test rig

Specification of the test rig is listed in Table 1.

### FEM analysis using ANSYS

To consider leakage effects and nonlinearity effects such as hysteresis of PM and saturation density of cores, we calculate the magnetic force with the variation of the displacement and the current using commercial FEM analysis program, ANSYS. Since PMMB has two dimensional shapes, analysis is performed with two dimensional models for convenience. The result of magnetic force with range of  $\pm 50\mu m$ ,  $\pm 1A$  is shown in Figure 6.

### EXPERIMENT OF 1-DOF TEST RIG

#### Configuration of test rig

For the performance test of PMMB, 1-Dof test rig is constructed from the result of magnetic circuit and FEM analysis. Linear motion guides and ball bush guarantee a linear motion of the test rig. A average of two eddy current sensor signals is used for control and additional mass can be attached. Figure 7 is a schematic diagram of 1-Dof test rig and Figure 8 is system configuration for control.

$$G(s) = \frac{K_I}{ms^2 - K_x} \quad (7)$$

#### Static load test

The weight of levitated moving part is supported by the magnetic force, which is a function of current and

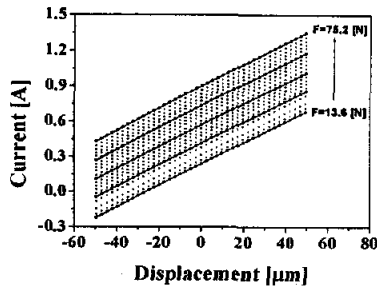


FIGURE 9: Experimental results for static load test current vs. force

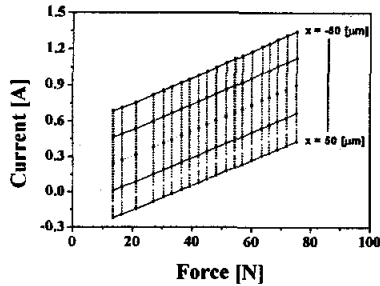


FIGURE 10: Experimental results for static load test displacement vs. force

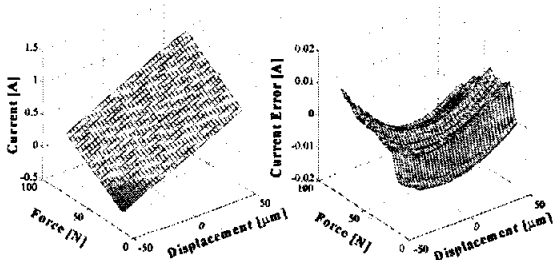


FIGURE 11: Experimental result of static load test – force vs. displacement vs. current and linearity error

displacement. Mass load, current and displacement have a relation described by (8) in steady state in servo control using feedback control.

$$F = mg = F(x, I) \quad (8)$$

In servo-control we vary displacement  $x$  from  $-50\mu\text{m}$  to  $50\mu\text{m}$  with step of  $5\mu\text{m}$  totally in 41 points and measure currents. This experiments are repeated 10 times for reliability.

Figure 9, 10 describe current variation according to mass load and displacement variations. The result of static load test shows the linear characteristics of PMMB force. If we assume (9) in the operation range, current stiffness  $K_I$  and displacement stiffness  $K_x$  can be calculated by Least Square Method or Minimum one Method.

$$F(x, I) = K_x x + K_I I + \Delta F \quad (9)$$

Figure 11 shows the result in three dimensions and linearity error of magnetic force.

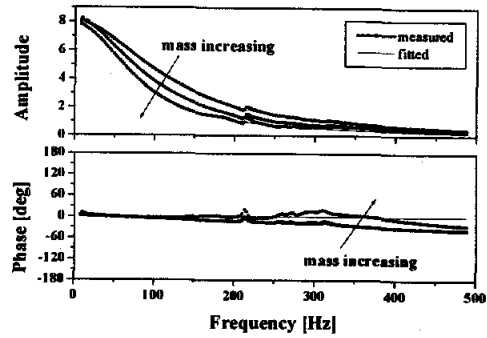


FIGURE 12: Frequency response function by mass variation

TABLE 2: Displacement and current stiffness

	Displacement Stiffness [N/ $\mu\text{m}$ ]		Current Stiffness [N/A]	
Magnetic Circuit Theory	-1.022	(100%)	102.3	(100%)
Finite Element Method	-0.9818	(96.8%)	101.6	(98.8%)
Static Load Test	-0.8503	(83.3%)	92.7	(90.8%)
Parameter Estimation	-0.7681	(75.2%)	88.0	(86.2%)

#### Parameter Identification by FRF

The current stiffness  $K_I$  and displacement stiffness  $K_x$  are estimated by the data interpolation in frequency domain. We put the sine wave input to the current signal of the MB and get FRF of  $G_{\text{exp}}(j\omega)$  by FFT analysis of input current  $I$  and displacement  $x$ . For reliability experiments are repeated five times with five kinds of mass. We assume the current stiffness  $K_I$  and displacement stiffness  $K_x$  is constant and estimate 2-norms of errors between FRF result and theoretical linear model.

$$G_i(j\omega) = -\frac{K_I}{(m + \Delta m_i)\omega^2 + K_x} \quad (i = 0 \sim N) \quad (10)$$

$$\arg \min_{K_x, K_I} \sum_{i=0}^N \sum_{\omega} \|G_i(j\omega) - G_{i, \text{exp}}(j\omega)\|_2^2$$

#### Comparison of Current and Displacement Stiffness

Table 2 compares the current stiffness  $K_I$  and the displacement stiffness  $K_x$  obtained by theoretical result and the experiment results and encloses relative values with 100% magnetic circuit.

#### Response experiment in time domain

We intended PMMB to use in high-precision position control. We added fine step references to general PID controller and acquire system responses in time domain. The raw signals of 50nm step response and the signals

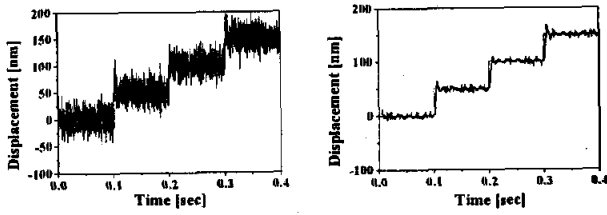


FIGURE 13: 50nm step response  
(Raw data and 300Hz low-pass filtered data)

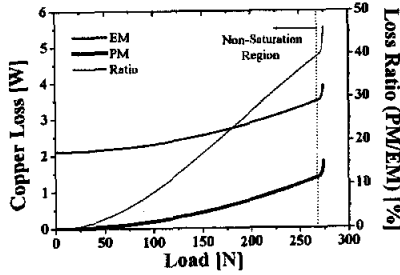


FIGURE 14: Comparison of copper loss

filtered by 300Hz low-pass filter are shown in figure 13. Stability time is 30ms and overshoot is 30%.

## COMPARISON OF POWER CONSUMPTION

### EM with the same performance

To compare power consumption of PMMB and electromagnetic bearing we assume electromagnetic bearing with E shaped core having the same coil turns, pole area, gap as that of PMMB. Magnetic density and linearized magnetic force is below.

$$\begin{bmatrix} B_1 \\ B_2 \end{bmatrix} = \frac{\mu_0 N}{2} \begin{bmatrix} I_b + I_c \\ g_0 - x \\ I_b - I_c \\ g_0 + x \end{bmatrix} \quad (11)$$

$$F = K_f \cdot I_c + K_x \cdot x$$

$$K_x = \frac{\partial f}{\partial x} = \frac{2\mu_0 N^2 I_b^2 A_g}{g_0^3}, \quad K_f = \frac{\partial f}{\partial I_c} = \frac{2\mu_0 N^2 I_b A_g}{g_0^2}$$

Since the electromagnetic bearing uses bias current to make nominal flux density, we compare two actuators by setting bias current of electromagnetic bearing making the same magnetic density.

$$(B_{nom})_{PM} = \frac{I_m B_r}{2 \left( g_0 + \frac{I_m}{\mu_m} \frac{A_g}{A_m} \right)} = \frac{\mu_0 N I_b}{2 g_0} = (B_{nom})_{EM} \quad (12)$$

By using calculated bias current in (12), current

stiffness  $K_f$  and displacement stiffness  $K_x$  are calculated such as (13) and they are the same as those of PMMB. So we can establish electromagnet bearing of the same performance.

$$(K_x)_{EM} = \frac{2\mu_0 N^2 I_b^2 A_g}{g_0^3} = \frac{2A_g B_r^2}{\mu_0 g_0 \left( \mu_m \frac{g_0}{I_m} + \frac{A_g}{A_m} \right)^2} = (K_x)_{PM} \quad (13)$$

$$(K_f)_{EM} = \frac{2\mu_0 N^2 I_b A_g}{g_0^2} = \frac{2N A_g B_r}{g_0 \left( \mu_m \frac{g_0}{I_m} + \frac{A_g}{A_m} \right)} = (K_f)_{PM}$$

### Comparison of power consumption

Energy consumption of MB consists of copper loss and iron loss. In case of linear magnetic bearing, since small perturbation is expected in steady state and laminated core is used, iron loss can be ignored. Copper loss is important loss factor and two kinds of MB has copper losses as below,

$$\begin{aligned} (E)_{PM} &= R \cdot I_c^2 + R \cdot I_c^2 = 2R I_c^2 \\ (E)_{EM} &= R \cdot (I_b + I_c)^2 + R \cdot (I_b - I_c)^2 = 2R(I_b^2 + I_c^2) \end{aligned} \quad (14)$$

Copper loss and loss ratio along to magnetic force is shown in Figure 14. In general operating range, a copper loss of PMMB is below 10% than that of electromagnetic bearing. Thus PMMB is suitable for high-precision actuator due to its low heat generation and high efficiency.

Considering the heat generation and cooling problem, the thicker coil is needed to allow large bias current with control current. So PMMB has increased suspension stiffness compared to conventional electromagnetic bearings with the same volume.

## 6-DOF LINEAR MOTION STAGE

With PMMB actuator, the operating range of the maglev motion stage will be highly increased due to improved linear characteristics and less influenced by the heat deformation problem and the repeatability of the whole system will be more improved to compensate the traveling errors of the maglev motion stage.

Magnetically levitated high-precision linear motion stage of 6-Dof motions is constructed for evaluating application characteristics of PMMB to stage. Stage has 4 magnetic bearing module (Figure 15), which consist of a PM biased magnetic bearing, a side EM bearing and 3 embedded capacitive sensors.

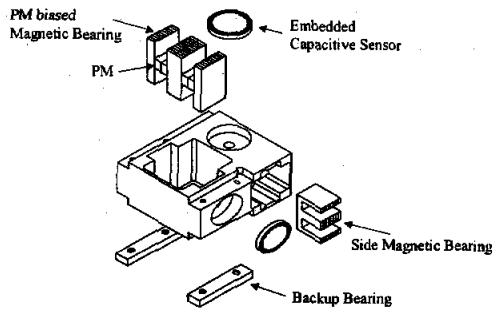


FIGURE 15: PM biased magnetic bearing module

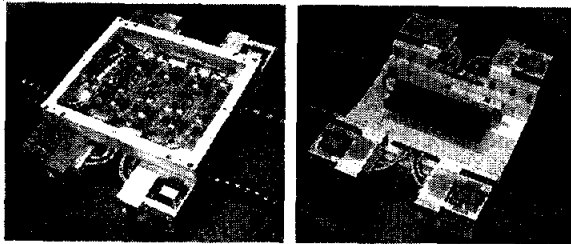


FIGURE 16: Linear Motion Stage  
(Left: upper view, Right: lower view)

The constructed 6-Dof stage has 400 $\mu$ m operating range, 50nm resolution along 100mm movement on 1-axis. The linear motor and linear encoder, which are located in lower part of stage, drive the motion on 1-axis.

Theoretical model has no off-diagonal term in frequency response function of the stage but actual stage has off-diagonal terms below 1.5%. Compared to theoretical model, it has some errors in high frequency but nearly equal. Time-lag of current amplifier or digital control and unknown effect of sensor, hysteresis, non-linearity may affect errors.

#### SUMMARY

We proposed that the novel permanent magnet biased linear magnetic bearing is suitable for the maglev high-precision motion stage due to its advantage over the conventional electromagnets – wide operation range, linearity, less heat generation etc. With this result, we designed and manufactured the maglev motion stage including four bearing modules composed of the novel permanent biased linear magnetic bearing suggested in this paper. The FRF response of stage is nearly resembled to theoretical model since new MB characteristics is well represented by linear equation.

#### References

1. S.C.Joung, Y.Joung, I.B.Chang, D.C.Han, "An experimental study on the high precision linear motion

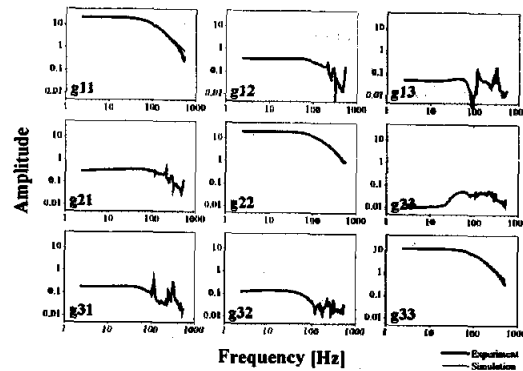


FIGURE 17: Frequency response function of the stage  
(Z, Roll, Pitch motion) – magnitude

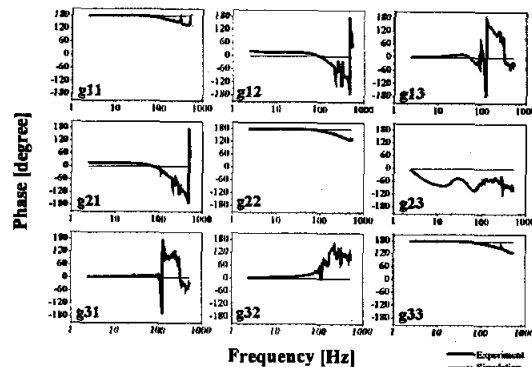


FIGURE 18: Frequency response function of the stage  
(Z, Roll, Pitch motion) - phase

table with magnetic bearing suspension", ASPE, USA, 1995, pp328-331

2. F.Auer, H.F. van Beek, "Practical Application of a magnetic bearing and linear propulsion unit for six degrees of freedom positioning", 4th Int. Symposium on Magnetic Bearings, August, 1994, ETH Zurich, pp183-188

3. M.Ruskowski, K.Popp, "Nonlinear modeling of a magnetically guided machine tool axis", 7th Int. Symposium on Magnetic Bearings, August 23-25, 2000, ETH Zurich, pp413-418

4. A.C.Lee, F.Z.Hsiao, D.Ko, "Analysis and testing of magnetic bearing with permanent magnets for bias", JSME Int. Journal, Vol.37, No.4, 1994

5. Arling, R.W. and Kohler, S.M., "Six Degree of Freedom Fine Motion Positioning Stage Based on Magnetic Levitation", 2<sup>nd</sup> International Symposium on Magnetic Suspension Technology, Seattle, WA, Aug. 11-13, 1993, pp.641-652